# MODELLING ELASTIC WALLS IN LATTICE BOLTZMANN SIMULATIONS FOR APPLICATIONS IN HAEMODYNAMICS

**X. Descovich[(a),(b)], G. Pontrelli[(c)], S. Melchionna[(c)], S. Succi[(c)], M. Bammer[(a)]**

[(a)]AIT Austrian Institute of Technology GmbH, Vienna, Austria
[(b)]Vienna University of Technology, Institute of Analysis and Scientific Computing, Vienna, Austria
[(c)]Consiglio Nazionale delle Ricerche, Rome, Italy

[(a),(b)]xenia.descovich.fl@ait.ac.at, [(c)]giuseppe.pontrelli@gmail.com, simone.melchionna@roma1.infn.it, s.succi@iac.cnr.it, [(a)]manfred.bammer@ait.ac.at

## ABSTRACT

An essential part in haemodynamic simulations is the incorporation of the arterial elasticity by modelling the interaction between the blood flow and the vessel wall. We suggest a simple approach for modelling elastic walls in lattice Boltzmann simulations of blood flow in an artery segment. It is based on state changes of the nodes (labelled as *fluid* and *solid*) of the underlying lattice. This change of node type models the displacement of the vessel wall and is dependent on the local pressure of the surrounding fluid nodes. The approach is combined with a continuous bounce-back boundary condition which ensures a more gradual displacement of the wall. We carried out numerical experiments on a portion of a vessel to show the feasibility of our approach. Compared to simulations without continuous bounce-back condition, the outcome of the simulations including it show smooth results.

Keywords: lattice Boltzmann method, fluid dynamics, elastic walls, continuous bounce-back condition

## 1. INTRODUCTION

Cardiovascular diseases are the most common cause of death in the European Union (Eurostat 2009). Thus, research in that domain has gained importance in the past years. Mathematical models and numerical methods are used to simulate the haemodynamic processes. Since arteries change in diameter depending on the pulsatile pressure inside, which is due to the periodicity of the heartbeat, it is of particular importance to incorporate this elasticity of the blood vessel in models of physiological flows, especially when considering vessels of large diameter.

Common numerical methods for simulations of the blood flow in elastic vessels are complex. Fang et al. (2002), for example, uses a parametrisation of the vessel wall with special treatment for curved boundaries. Their method has been successfully applied to unsteady flows in elastic tubes in two dimensions by Hoekstra et al. (2004). However, the method is very complex in three dimensions because the vessel wall is described by means of surfaces.

We have developed a simple approach for modelling the elastic wall for which no parametrisation is needed. We have performed our simulations in two dimensions, but the method can easily be extended to three dimensions.

The remainder of this paper starts with a short overview of the lattice Boltzmann method and its application to haemodynamics in Section 2. In Section 3, we give a detailed description of the method to model the elastic vessel wall, describing its spatial displacement as it interacts with the flow dynamics. Section 4 presents results of numerical experiments and compares two kinds of boundary conditions for the wall boundaries. Section 5 gives an outlook on the possible application of the method in haemodynamics. A short conclusion in Section 6 sums up the presented results.

## 2. LBGK METHOD FOR BLOOD FLOW SIMULATION

The lattice Boltzmann (LB) method is a mesoscopic approach based on the Boltzmann equation from statistical mechanics. It describes the evolution of fictitious particles on nodes of a regular lattice. The main variables are density distribution functions $f_i(\vec{x},t) = f(\vec{x},\vec{c}_i,t)$ (also called *populations*) which denote the probability of finding at time $t$ a particle located at site $\vec{x}$ and travelling along the lattice links in direction $i$ with the speed $\vec{c}_i$. Starting from an initial state, the populations evolve at every time step in two consecutive sub-steps: (a) *collision*, describing the interaction of particles at a node, and (b) *streaming* (*propagation*), in which each particle is propagated to the neighbouring node based on the direction of its velocity. A more detailed introduction to the LB method can be found in the books of Wolf-Gladrow (2000) and Succi (2001).

The LB method is a valuable alternative to numerical methods that are based on the solution of the Navier-Stokes equations of continuum mechanics. Many authors have successfully applied lattice Boltzmann models in haemodynamics (Fang et al. 2002, Artoli 2003, Leitner 2007, Pontrelli et al. 2009, Melchionna et al. 2010).

Considering large arteries only, the flow is assumed to be Newtonian. For our simulations of the blood flow, we use a D2Q9 model (two spatial dimensions, nine directions $i$; see Fig. 1). The dynamics of the flow field are computed on the basis of the lattice Boltzmann equation with single-time relaxation and linearised collision operator (LBGK approximation)

$$f_i(\vec{x} + \vec{c}_i\Delta t, t + \Delta t) - f_i(\vec{x}, t) = -\omega\Delta t\left(f_i(\vec{x}, t) - f_i^{eq}(\rho, \vec{u})\right) \quad (1)$$

with $\Delta t$ being the temporal resolution and $\omega$ being the relaxation frequency. The right-hand side of equation (1) represents molecular collisions through a relaxation towards a local equilibrium $f_i^{eq}$ which is given by a second-order expansion of the Maxwell-Boltzmann distribution. The fluid density $\rho$ and the momentum $\rho\vec{u}$ are defined based on the distribution functions $f_i$:

$$\rho = \sum_{i=0}^{8} f_i \quad (2)$$

$$\rho\vec{u} = \sum_{i=0}^{8} f_i\vec{c}_i \quad (3)$$

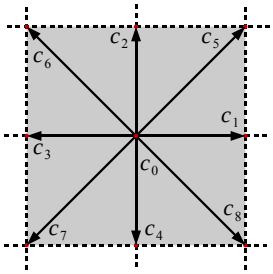


Figure 1: D2Q9 lattice

## 3. MODELLING THE ELASTIC WALL

In simulations of the blood flow in larger vessels, it is important to include the compliance of the vessel. We have developed a simple approach to model the elastic vessel which does not need a parametrisation of the wall. Our modelling is based on the work of Leitner (2007) and acts strictly locally as the LB method itself. By this, the complexity of the algorithm is not increased.

### 3.1. Displacement of Wall Based on Node Type Changes

In our modelling of the vessel wall, the nodes of the lattice can have two different states: *fluid*, representing the blood inside the vessel, and *solid*, denoting the tissue of the vessel. Contrary to the modelling described by Leitner (2007), the vessel wall is not situated on the solid nodes but is located between fluid and solid nodes in a given direction. All nodes that are not fluid are by default solid. Our approach does not require cellular automata used in Leitner's method to avoid a rupture of the vessel wall. The displacement of the wall is modelled by changing the type of a node – from solid to fluid for an outwards displacement (expansion) and vice versa for an inwards displacement (contraction). The change of node type is dependent on the local pressure of the surrounding fluid nodes.

#### 3.1.1. Initialization of New Fluid Nodes

New fluid nodes need to be initialized with values of the density ρ and the velocity $\vec{u}$ which are computed based on the populations $f_i$ from the neighbouring fluid nodes.

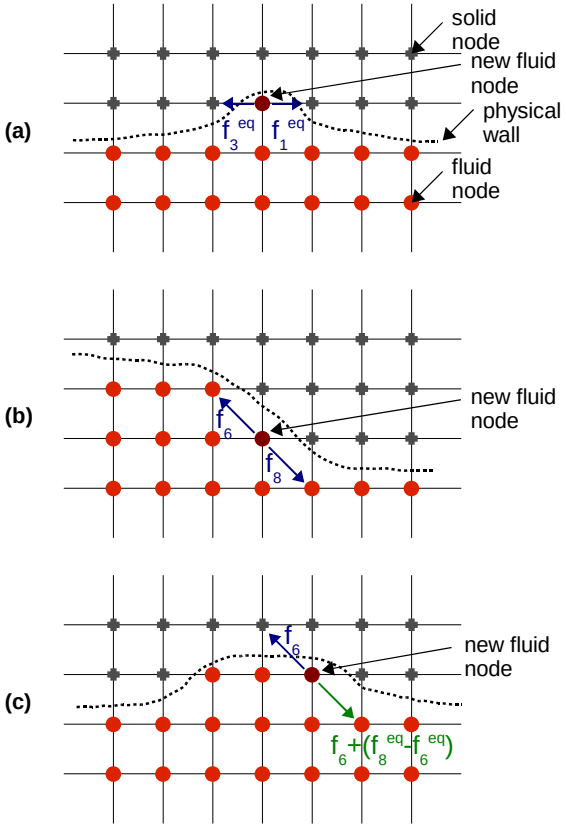


Figure 2: Sketch of lattice illustrating the initialization of new fluid nodes (dark red disks). (a) Example of a new fluid node having solid neighbours in direction 1 and 3. (b) Example of a new fluid node having fluid neighbours in direction 6 and 8. (c) Example of a new fluid node having a fluid neighbour in direction 8 and a solid neighbour in opposite direction.

When determining the populations $f_i$ at the new fluid node $(x, y)$, three cases can occur: (a) If the neighbouring nodes of $(x, y)$ in direction $i$ and opposite direction $i'$ are both solid, $f_i$ and $f_{i'}$ are set to their equilibrium value $f_i^{eq}$ and $f_{i'}^{eq}$, respectively. (b) If the neighbouring nodes of $(x, y)$ in direction $i$ and $i'$ are both fluid, $f_i$ and $f_{i'}$ are gained from propagation. (c) If the neighbouring node of $(x, y)$ in direction $i$ is fluid and the neighbouring node of $(x, y)$ in direction $i'$ is solid, $f_{i'}$ is gained from propagation and $f_i$ is calculated using the bounce-back rule for the non-equilibrium part of the distribution function $f_i$ $(f_i = f_{i'} + (f_i^{eq} - f_{i'}^{eq})$, see Zou and He, 1997). Fig. 2 illustrates this initialization procedure.

Compared to the method of Leitner (2007), who initializes new fluid nodes with an equilibrium distribution function, this procedure includes also the non-equilibrium part of the populations, which is not negligible in proximity of the wall.

A mass conservation problem arises when nodes change their type because the total number of fluid nodes changes. Mass is a priori not conserved as mass is added when initializing new fluid nodes or subtracted when a node changes its state from fluid to solid. Leitner (2007) does not refer to this issue, and it is not clearly evident how it is circumvented. In order to ensure mass conservation, we have developed methods that rescale the LB populations in a part of the domain when a node type change occurs and so ensure mass conservation. For more details, the reader is referred to our previous work (Descovich et al., 2012).

#### 3.1.2. Continuous Bounce-Back Boundary Condition

For the wall boundaries, the bounce-back scheme in combination with spatial interpolation is applied. A linear interpolation (Bouzidi et al., 2001) is used to determine the unknown distribution functions near the wall with directions pointing into the fluid domain.

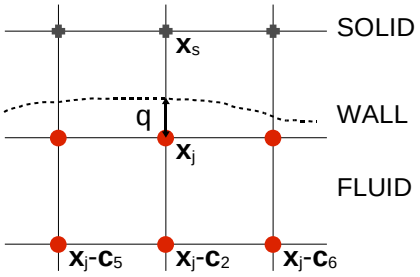


Figure 3: Illustration for the continuous bounce-back boundary condition for a virtual wall located at distance $q$ from the last fluid node. Gray crosses indicate solid nodes; red filled circles denote fluid nodes. The lattice spacing $\Delta x$ is set to one.

The wall is imagined to be located at a certain distance q from the last fluid node, see Fig. 3. The lattice spacing $\Delta x$ is set to one; thus, q ranges between zero and one. If $q = 1/2$, the normal bounce-back rule is recovered (halfway bounce-back on the link). The following scheme is applied to all links that cross the imaginary wall. Let $\vec{x}_j$ be a fluid node such that $\vec{x}_s = \vec{x}_j + \vec{c}_i$ is a solid node and let $i'$ denote the opposite direction of $i$ (thus, $\vec{c}_{i'} = -\vec{c}_i$). For the unknown distribution functions at node $\vec{x}_j$, the following linear interpolation is used.

$$f_{i'}(\vec{x}_j, t+1) = 2q f_i^*(\vec{x}_j, t) + (1-2q) f_i^*(\vec{x}_j - \vec{c}_i, t), \quad q < \frac{1}{2} \tag{4}$$

$$f_{i'}(\vec{x}_j, t+1) = \frac{1}{2q} f_i^*(\vec{x}_j, t) + \frac{(2q-1)}{2q} f_{i'}^*(\vec{x}_j, t), \quad q \geq \frac{1}{2} \tag{5}$$

Here, the superscript $*$ denotes the post-collisional state and $\Delta t$ has been set to one.

In the simulation, two arrays of $q$-values are used, one for the lower and one for the upper boundary. Thus, for every fluid node $(x, y_b)$ next to a boundary, $q_b(x) = q(x, y_b)$ determines the distance from node $(x, y_b)$ to the wall. Here, the subscript in $y_b$ specifies whether the lower boundary ($b = lower$) or the upper boundary ($b = upper$) is considered. For the sake of simplicity, the subscript is omitted in cases in which it is not necessary to specify which boundary is considered.

The parameter $q$ of a certain node next to the boundary is linked to the pressure at this node. More details about the exact relationship between $q$ and the pressure are described further down. The approach of coupling $q$ with the pressure and using continuous bounce-back boundary conditions at the wall allows a more gradual displacement of the (virtual) wall instead of moving the vessel wall by one lattice unit within a single time step.

### 3.2. Pressure Thresholds

The change of node type is dependent on the local pressure surrounding a considered node. Pressure thresholds are assigned to each node, increasing with the radius of the vessel segment. Nodes located further away from the centre of the vessel have a higher threshold so that a higher pressure is needed for an outwards displacement of the wall, i.e., for changing the type of a node from solid to fluid.

For our simulations, we assume a linear relationship between the pressure $p$ and the radius $R$, similar to the one of the pulmonary blood vessels (see Fung 1997):

$$p = p_0 + \alpha(R - R_0) \tag{6}$$

Here, α is a compliance constant. $R_0$ is the radius when the transmural pressure is zero and $p_0$ denotes the pressure at a node located at distance $R_0$ from the centre of the vessel. The excess of pressure $(p - p_0)$ is needed to induce the wall displacement $(R - R_0)$. The relation above is a good approximation for large arteries (Hoekstra et al. 2004).

The pressure thresholds are computed based on this linear relationship and assigned to each node. The criterion for changing the type of a node is related to the parameter $q$ of the continuous bounce-back boundary condition and will be explained in the next section.

### 3.3. Coupling between Pressure Threshold and Parameter $q$

The parameter $q$ is related to the pressure in the following way. Let $p(x, y_b)$ denote the current pressure

at a fluid node $(x, y_b)$ directly next to the wall and $p_{th}(x, y_b)$ the pressure threshold at this node. The difference to the pressure threshold of the neighbouring node (in $y$-direction) is given by the parameter α in the linear pressure-radius relationship, see Eq. (6). At every time step, the parameter $q$ is updated based on the following relationship.

$$q(x, y_b) = \frac{p(x, y_b) - p_{th}(x, y_b)}{\alpha} \quad (7)$$

$q$ changes at every time step at each $x$ because it is related to the pressure which varies in time. $q$ increases as $p$ increases and, vice versa, $q$ decreases as $p$ decreases. The value of $q$ determines whether a node type change occurs or not. If $q$ becomes greater than one because of a large pressure increase (thus, $p(x, y_b) - p_{th}(x, y_b) > \alpha$), the solid node next to the considered fluid node $(x, y_b)$ changes its state to fluid. On the contrary, if $q$ falls below zero because of a large pressure decrease ($p(x, y_b) < p_{th}(x, y_b)$), the node $(x, y_b)$ changes its state from fluid to solid.

As soon as a node type change occurs (which happens when $q > 1$ or $q < 0$), $q$ has to be reset to a value between zero and one. This is done in the following way. If $q$ exceeds one, thus $q = 1 + \Delta q$ with $\Delta q > 0$, the new $q$ is set to $\Delta q$ if $\Delta q < 1$ and set to one if $\Delta q > 1$. In a similar way, if q falls below zero, thus $q = -\Delta q$ with $\Delta q > 0$, the new q is set to $(1 - \Delta q)$ if $\Delta q < 1$ and to zero if $\Delta q > 1$.

The described approach allows a continuous displacement of the vessel wall. The populations at a node next to the wall are corrected many times before the node changes its state. As a consequence, the system is less perturbed when a node type change occurs.

## 4. SIMULATION RESULTS

We have implemented a simulation code for the lattice Boltzmann algorithm combined with our model for the elastic wall using the programming language C.

For our simulations, we consider an initially straight channel modelling the vessel which is embedded in a computational domain of fixed dimensions $N_x \times N_y$, where $N_x$ and $N_y$ are the number of lattice nodes (equally spaced) in direction $x$ and $y$, respectively. At inlet and outlet, we impose pressure boundary conditions using the method of Zou and He (1997) to determine the unknown LB populations pointing into the fluid domain. At the inlet, we prescribe an oscillating pressure. This is equivalent to imposing an oscillating density because density $\rho$ and pressure $p$ are linearly related through $p = c_s^2 \rho$, where $c_s^2$ is the sound of speed. For simplicity, the pressure at the outlet is set constant. It is chosen in a way that the pressure gradient between inlet and outlet is always positive. At the wall, we impose the continuous bounce-back boundary condition described above, which represents a no-slip condition (i.e., the fluid velocity is zero at the wall). Expansion and contraction are allowed only after 1000 time steps when the flow is fully developed.

The following physical and numerical parameters have been used in the simulations: viscosity $\nu = 1/3$, initial density $\rho_0 = 1.0$, $\alpha = 0.007$, $p_0 = 1/3$, and $R_0 = 20$. All parameters and variables are normalized and thus dimensionless. A channel modelling the vessel of initial dimensions $200 \times 40$ nodes is embedded in the computational domain of fixed dimensions $200 \times 100$ nodes.

The oscillating density $\rho_{in}$ at the inlet is set to

$$\rho_{in} = \rho_{mean} + A \sin\left(\frac{2\pi t}{T_{pulse}}\right) \quad (8)$$

Here, $\rho_{mean} = 1.025$ is the mean pressure, $A = 0.025$ the amplitude of the oscillations, $t$ the time, and $T_{pulse} = 2500$ the period of the pulse. The density at the outlet, $\rho_{out}$, is set to one. Thus, the density difference between inlet and outlet varies between zero and 0.05.

### 4.1. Results with Halfway Bounce-Back on the Link Condition

In a first experiment, we have not included the continuous bounce-back boundary condition. Instead, we have used a halfway bounce-back on the link boundary condition. This means that the wall is located halfway between fluid and solid nodes. Since the distance $q$ from the last fluid node to the wall is constant ($q = 1/2$) in the case of the bounce-back on the link boundary condition, another condition for changing the type of a node has to be chosen. One possibility is to simply compare the current pressure to the pressure threshold and change the state of a node when the pressure exceeds or falls below the corresponding pressure threshold. As soon as the pressure at a fluid node exceeds the pressure threshold, the neighbouring solid node becomes fluid and the wall changes by one lattice unit within one single time step.

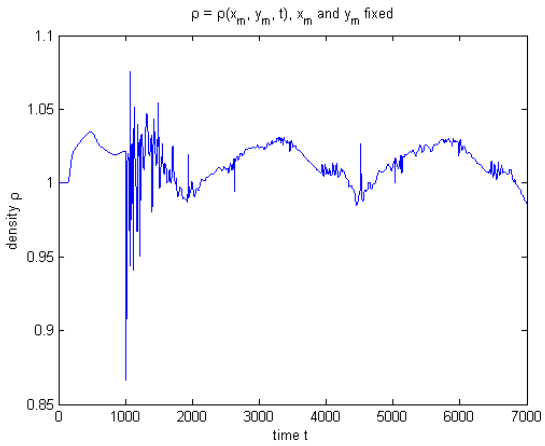


Figure 4: Density $\rho$ as a function of time at a node near the wall (bounce-back on the link)

Analogously, as soon as the pressure of a fluid node falls below the pressure threshold, the considered node becomes solid and the wall is displaced by one lattice

unit. Thus, the displacement of the wall is not continuous. The radius can only change by one full lattice unit.

Fig. 4 shows the density as a function of time at a fluid node near the wall. The time history of the velocity component $u_x$ at a node near the wall is depicted in Fig. 5. It can be observed that density and velocity oscillate in a correct way as a response to the oscillating pressure at the inlet, but are superposed by smaller oscillations and also display peaks that seem unphysical. These oscillations and peaks are caused by the discrete nature of the method due to the not continuous displacement of the wall which perturbs the system. The condition for changing the type of a node has been adapted again. In order to not use incorrect values of the pressure (that are just the consequence of the perturbation at the wall due to the node type change) for the comparison, the pressure over a certain number of time steps is averaged, and this average value is compared to the pressure threshold. This procedure avoids that the wall is displaced due to unphysical values of the pressure. However, the oscillations and peaks remain.

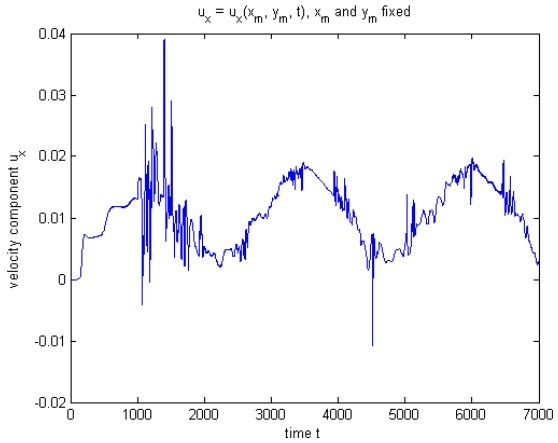


Figure 5: Velocity component $u_x$ as a function of time at a node near the wall (bounce-back on the link)

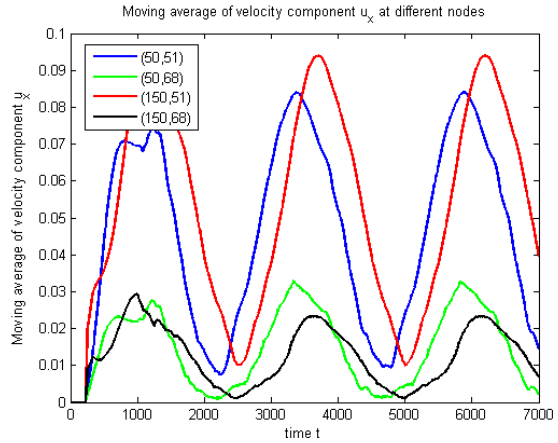


Figure 6: Moving average over 250 time steps of the velocity component $u_x$ at different lattice nodes (blue and red for a node with central $y$-coordinate, green and black for a node with $y$-coordinate near the upper wall)

Fig. 6 displays the moving average over 250 time steps (one tenth of the pulse period $T_{pulse}$) of the velocity component $u_x$ at different nodes of the channel. It can be observed that taking the moving average filters out the superposed oscillations and peaks appearing in the time history of the velocity. This underlines the assumption that the system reacts in a correct way and that the perturbations are only caused by the instantaneous displacement of the wall by one lattice unit.

### 4.2. Results with Continuous Bounce-Back Condition

In order to minimize the unphysical oscillations and spikes appearing in the time histories of the density and the velocity, we have run simulations including the continuous bounce-back boundary conditions.

Fig. 7 and 8 display the density $\rho$ and the velocity component $u_x$ as a function of time at a fluid node near the wall, respectively.

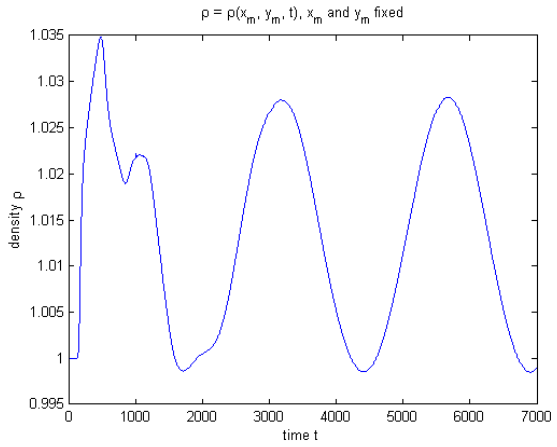


Figure 7: Density $\rho$ as a function of time at a node near the wall (continuous bounce-back)

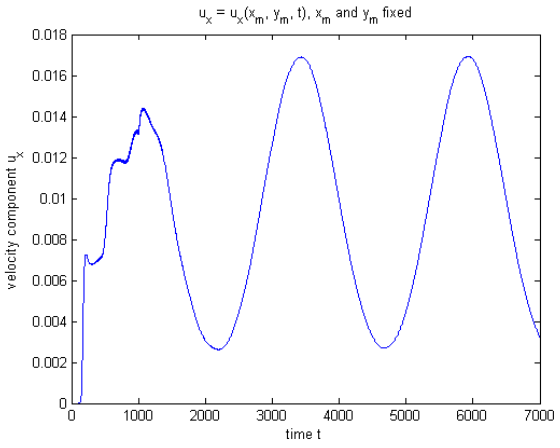


Figure 8: Velocity component $u_x$ as a function of time at a node near the wall (continuous bounce-back)

The time histories of $\rho$ and $u_x$ show smooth behaviour without superposed oscillations or spikes. This is due to the continuous displacement of the wall and to the fact that the LB populations are corrected

over several time steps before a node type change occurs and new fluid nodes are initialized based on the LB populations of the neighbouring nodes.

In order to study the behaviour of the wall, we have run simulations with different values of $\alpha$. Fig. 9 depicts the maximum radius as a function of the compliance parameter $\alpha$. As expected, a lower value of $\alpha$ leads to a larger deformation of the channel.

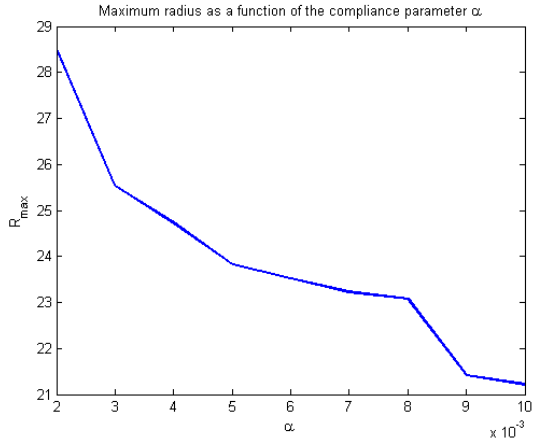


Figure 9: Maximum radius as a function of the compliance parameter $\alpha$

At the outlet, the channel is constrained due to the boundary condition which imposes a constant pressure. Since the pressure at the outlet does not change, the parameter $q$ does not change either and, as a consequence, the radius at the outlet is constant. In order to neglect the effect of the constriction of the outlet on the flow field, the channel has to be long enough. We are currently working on elaborating a physically more correct boundary condition that does not bound the outlet section. The results will be reported in a later work.

## 5. OUTLOOK

The aim of our future work is to apply the presented method to haemodynamics; in particular, we focus on the simulation of blood flow in stented arteries. A stent is a wire metal mesh that is inserted into a narrowed blood vessel to prevent its occlusion. The modelling of the elastic wall presented in this work has the advantage that it can also be applied to stented arteries with the only difference that nodes corresponding to the stented part will have higher pressure thresholds because this part is stiffer than the rest of the vessel.

## 6. CONCLUSION

We have developed a simple approach for modelling elastic walls in lattice Boltzmann simulations which can be applied to study the blood flow in arterial segments. We have carried out numerical experiments on a vessel model. The results show correct physical behaviour of the system and prove the feasibility of our approach.


## ACKNOWLEDGMENTS

This research was accomplished within the context of the project 'BioCompatible Materials and Applications – BCMA' initiated by the AIT Austrian Institute of Technology GmbH. It was partly funded by the AIT and the federal state of Lower Austria and co-financed by the EC (EFRE).


## REFERENCES


Artoli, A., 2003. *Mesoscopic computational haemodynamics*. Thesis (PhD). University of Amsterdam.

Bouzidi, M., Firdaouss, M., and Lallemand, P., 2001. Momentum transfer of a Boltzmann-lattice fluid with boundaries. *Physics of Fluids*, 13, 3452.

Descovich, X., Pontrelli, G., Succi, S., Melchionna, S., Bammer, M., 2012. Modeling elastic walls in lattice Boltzmann simulations of arterial blood flow. *Preprints of MATHMOD 2012 Vienna – Abstract Volume*, p. 265. February 15-17, 2012, Vienna (Austria).

Eurostat, 2009. *Health Statistics – Atlas on mortality in the European Union*. Luxemburg: Office for Official Publications of the European Communities.

Fang, H., Wang, Z., Lin, Z., and Liu, M., 2002. Lattice Boltzmann method for simulating the viscous flow in large distensible blood vessels. *Physical Reviews E*, 65 (5), 51925.

Fung, Y., 1997. *Biomechanics: Circulation*. Springer Verlag.

Hoekstra, A., van't Hoff, J., Artoli, A., and Sloot, P., 2004. Unsteady flow in a 2D elastic tube with the LBGK method. *Future Generation Computer Systems*, 20 (6), 917–924.

Leitner, D., 2007. *Simulation of Arterial Blood Flow with the Lattice Boltzmann Method*. Thesis (PhD). Vienna University of Technology.

Melchionna, S., Bernaschi, M., Succi, S., Kaxiras, E., Rybicki, F., Mitsouras, D., Coskun, A., and Feldman, C., 2010. Hydrokinetic approach to large-scale cardiovascular blood flow. *Computer Physics Communications*, 181 (3), 462–472.

Pontrelli, G., Ubertini, S., and Succi, S., 2009. The unstructured lattice Boltzmann method for non-Newtonian flows. *Journal of Statistical Mechanics: Theory and Experiment*, 6, P06005.

Succi, S., 2001. *The Lattice Boltzmann Equation*. Oxford: Oxford University Press.

Wolf-Gladrow, D., 2000. *Lattice-Gas Cellular Automata and Lattice Boltzmann Models: An Introduction*. Springer.

Zou, Q., and He, X., 1997. On pressure and velocity boundary conditions for the lattice Boltzmann BGK model. *Physical Fluids*, 9, 1591–1598.